

Electronic Supplementary Information (ESI)

Title: Super LCST Thermo-responsive Nanoparticle Assembly for ATP Binding
through Hofmeister Effect

Authors: Smita Kashyap and Manickam Jayakannan*¹

¹ E-mail: jayakannan@iiserpune.ac.in

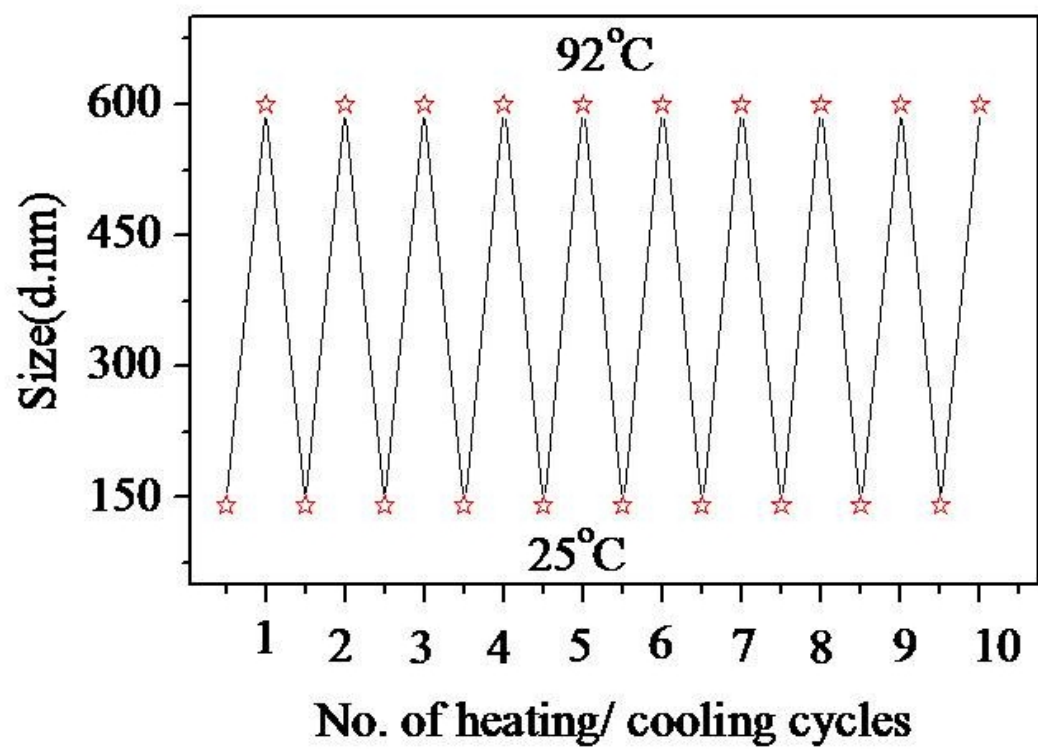


Figure SF-1. Hydrodynamic diameter oscillation of the nanoparticles in the heating and cooling cycle.

Note: The hydrodynamic diameter of the amphiphile in water was recorded at temperature above and below LCST in ten consecutive cycles. The plot reveals that the change in size of the nanoparticles from 140nm (below LCST) to 600 nm (above LCST) was completely reversible in nature.

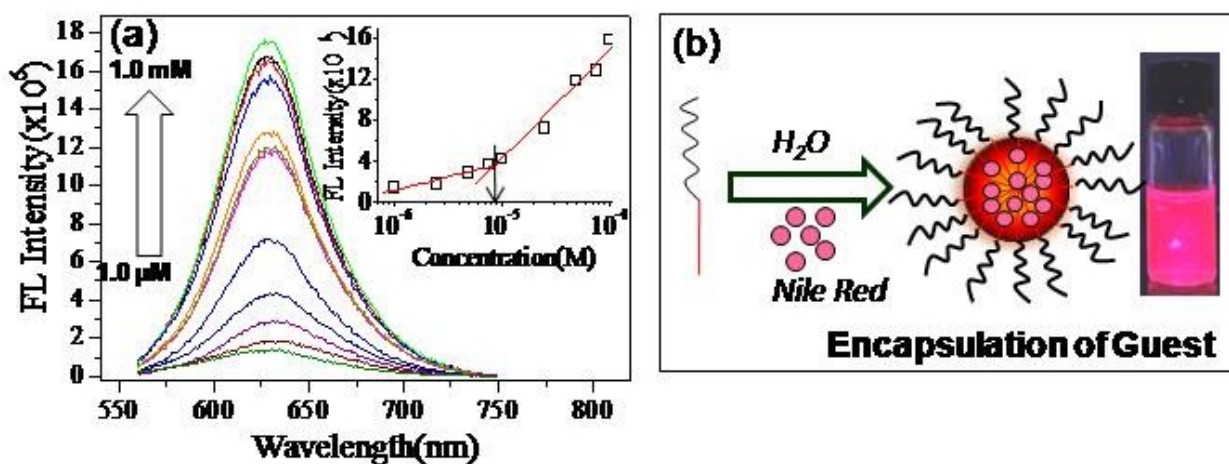


Figure SF-2 (a) Fluorescence spectra of Nile red (0.2 μM) encapsulated at concentration of amphiphile **1** from 1.0 μM to 1.0 mM. Inset figure show the plot of the emission intensity versus concentration of amphiphile **1** with a break point for CAC. (b) Schematic representation of Nile Red encapsulated micellar-nanoparticle of amphiphile **1** and photographs of vial represents the Nile red loaded scaffold in water.

Note: The plot reveals that CAC of amphiphile **1** is 1.0×10^{-5} M. The encapsulation efficiency of the amphiphile **1** for nile red was calculated using the formula given below:

$$\text{DLE}(\%) = \left\{ \frac{\text{weight of encapsulated nile red}}{\text{weight of nile red in feed}} \right\} \times 100\%.$$

And the efficiency of the amphiphile **1** with respect to nile red was found to be 1.7%.

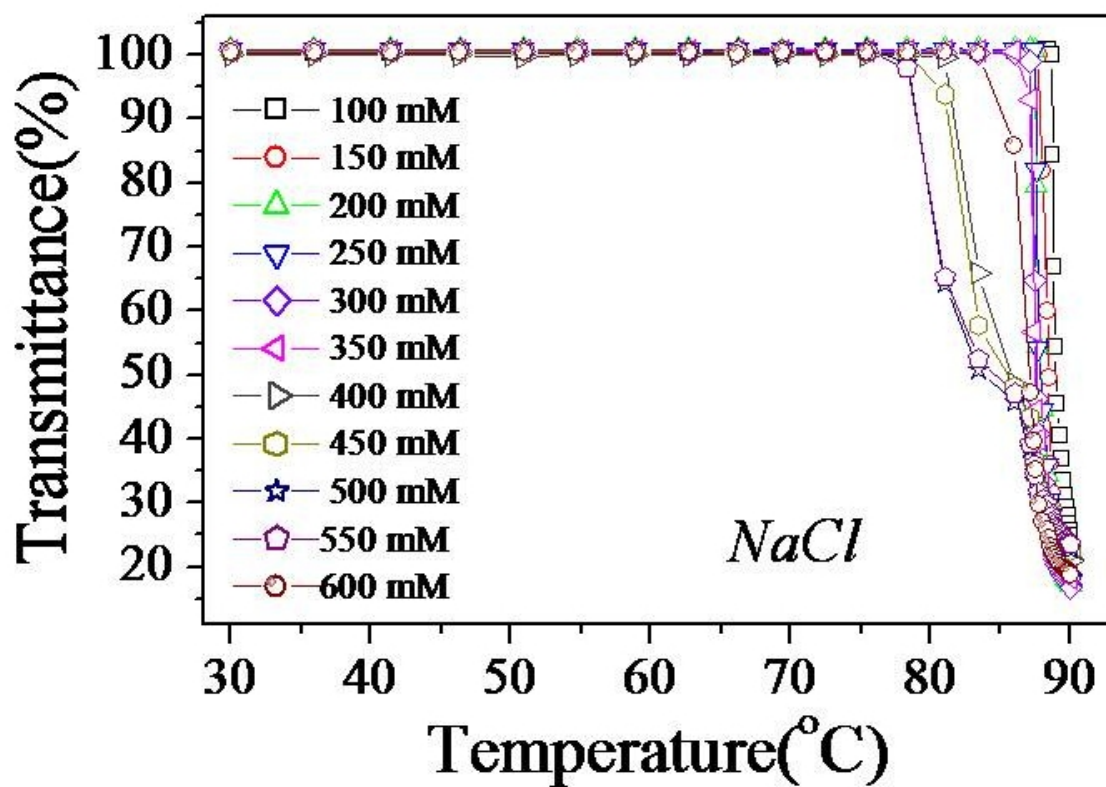


Figure SF-3. %Transmittance of amphiphile 1 (10^{-4} M) at various concentrations of sodium chloride (heating cycle).

Note: The plot reveals that with increase in the concentration of NaCl from 100 mM to 600 mM the LCST of the amphiphile 1 lowers down by 15 °C. This indicates that amphiphile 1 has less affinity towards Cl⁻ anion.

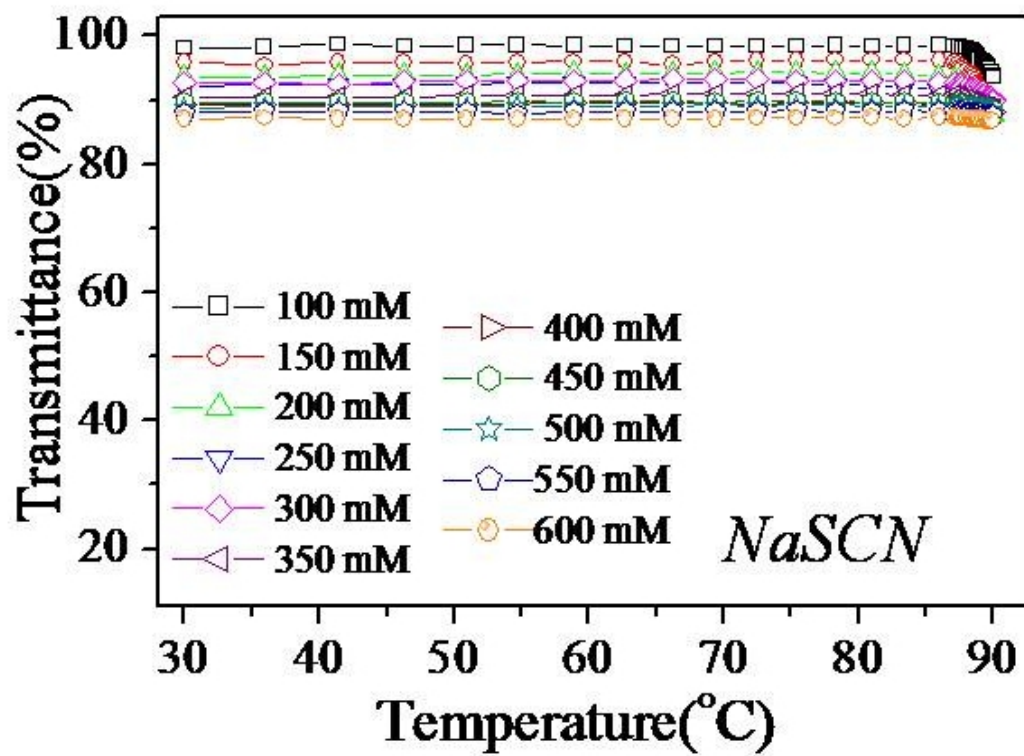


Figure SF-4. %Transmittance of amphiphile **1** (10^{-4} M) at various concentrations of sodium thiocyanate (heating cycle).

Note: From the plot it is evident that amphiphile **1** does not undergo phase-separation in presence of NaSCN thereby, indicating that NaSCN shows salting in behavior.

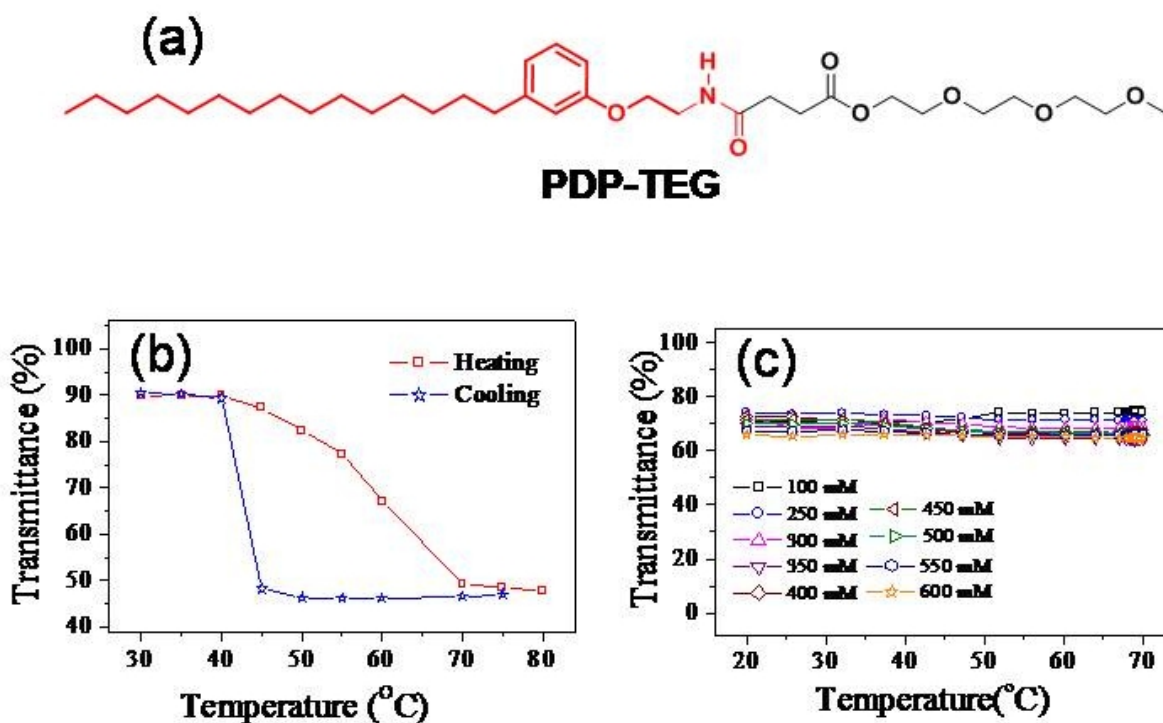


Figure SF-5. %Transmittance of thermo-responsive diblock having triethylene glycol (PDP-TEG) (a) absence of anions (b) at various concentrations of inorganic phosphate anion (Pi) (heating cycle). The plot of PDP-TEG was taken from our earlier work for comparison purpose (Smita and Jayakannan, *J. Mater. Chem. B*, 2014, **2**, 4142-4152).

Note: The aqueous solution of PDP-TEG (10^{-4} M) was subjected for the optical transmittance measurement in absence as well as in presence of various concentration of inorganic phosphate anion. The plot reveals that PDP-TEG shows LCST at 42° C in absence of anions while it does not undergo phase-separation in presence of inorganic phosphate anion. Thus, it does not exhibit Hofmeister effect.

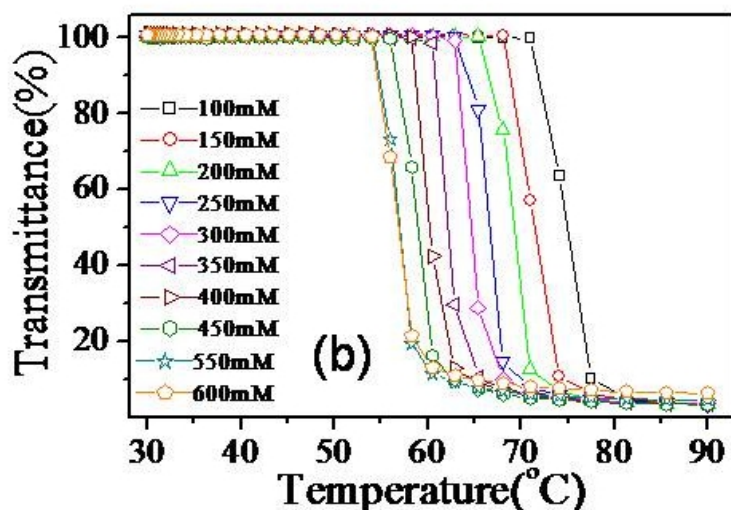
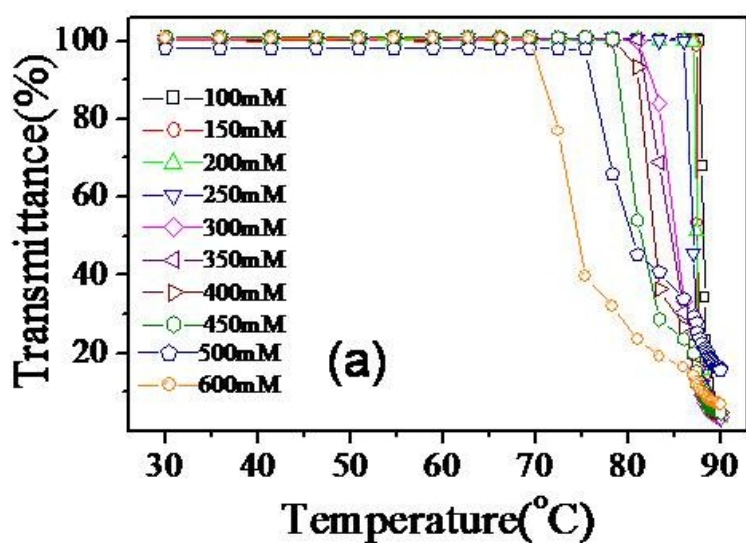


Figure SF-6. %Transmittance of amphiphile **1** (10^{-4} M) at various concentrations of inorganic phosphate anion (Pi) (a) Heating cycle (b) Cooling Cycle.

Note: From the heating cycle data it is evident that the LCST of amphiphile **1** decreases from 90 °C to 70 °C with the increase in the concentration of inorganic phosphate anion from 100 mM to 600 mM. Thus, LCST of amphiphile **1** gets lower down by 20 °C. Further, upon comparing the heating and cooling cycle data one can deduce that both heating and cooling process do not follow the same kinetic path.

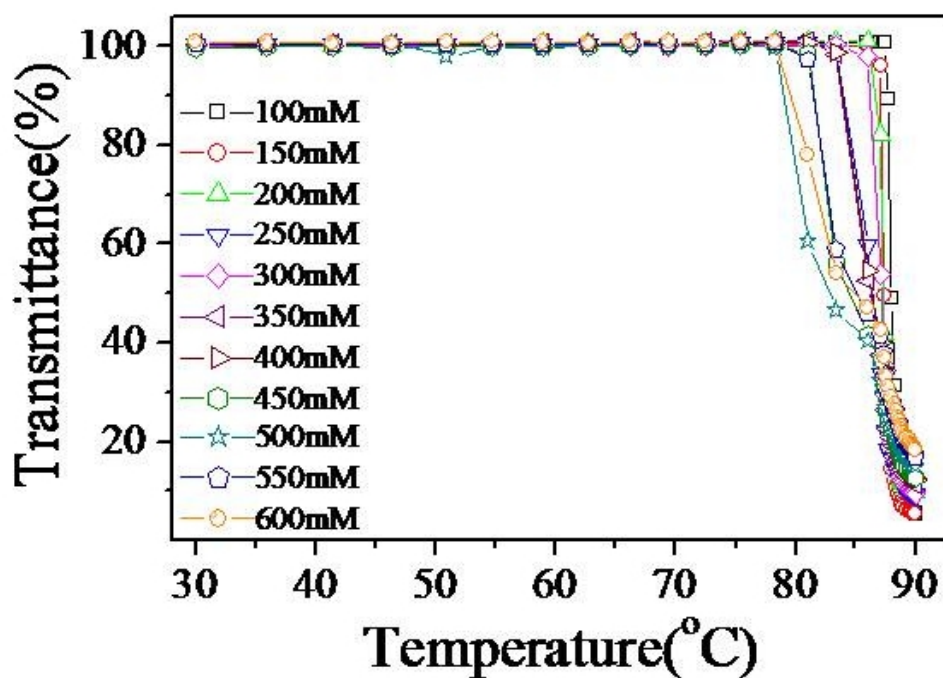


Figure SF-7. %Transmittance of amphiphile **1**(10^{-4} M) at various concentrations of Adenosine diphosphate (ADP).

Note: With increase in the concentration of ADP from 100 mM to 600 mM the LCST of the amphiphile **1** changes only by 15 °C. Thus, the amphiphile **1** has low affinity towards ADP.

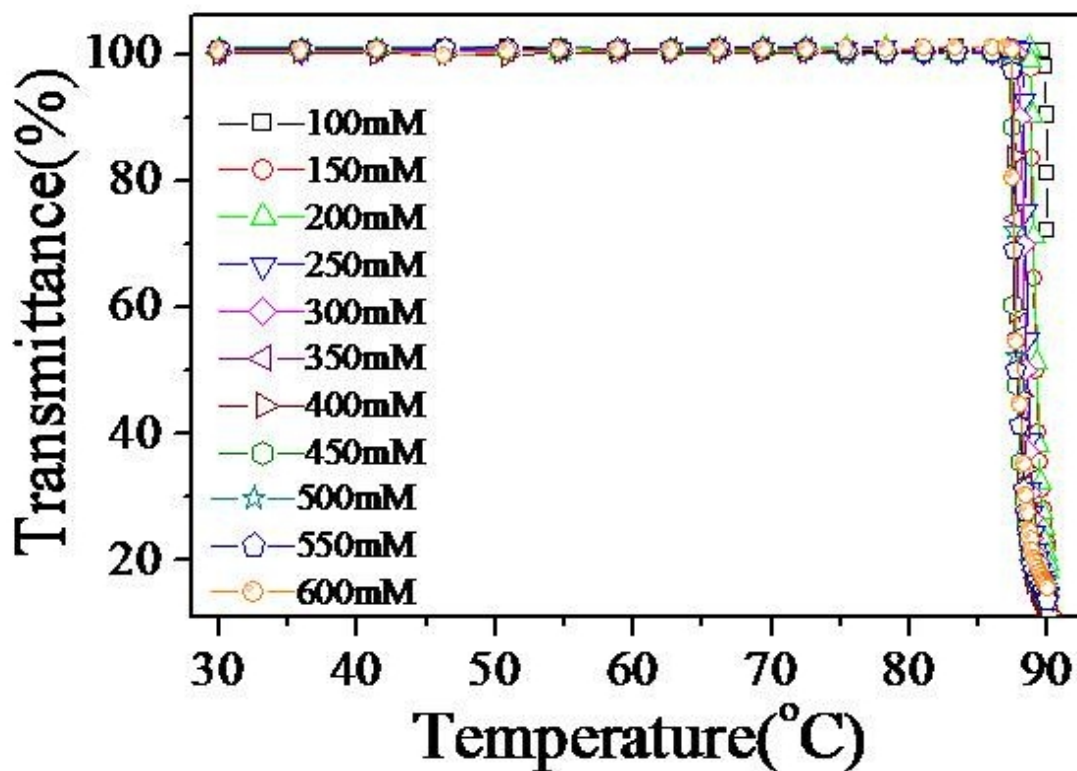


Figure SF-8. %Transmittance of amphiphile **1**(10^{-4} M) at various concentrations of Adenosine monophosphate (AMP).

Note: With increase in the concentration of AMP from 100 mM to 600 mM the LCST of the amphiphile **1** changes only by 5 °C. Therefore, presence of AMP does not lead to remarkable changes in the LCST of the amphiphile **1**.

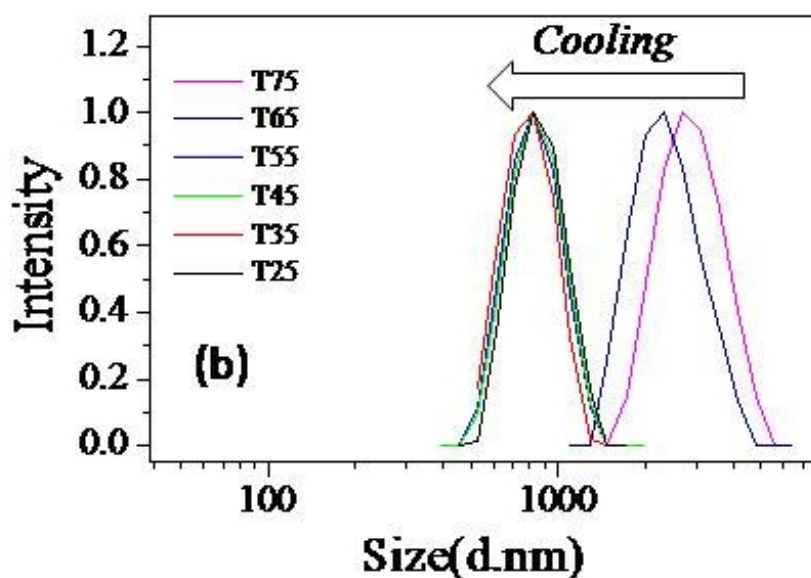
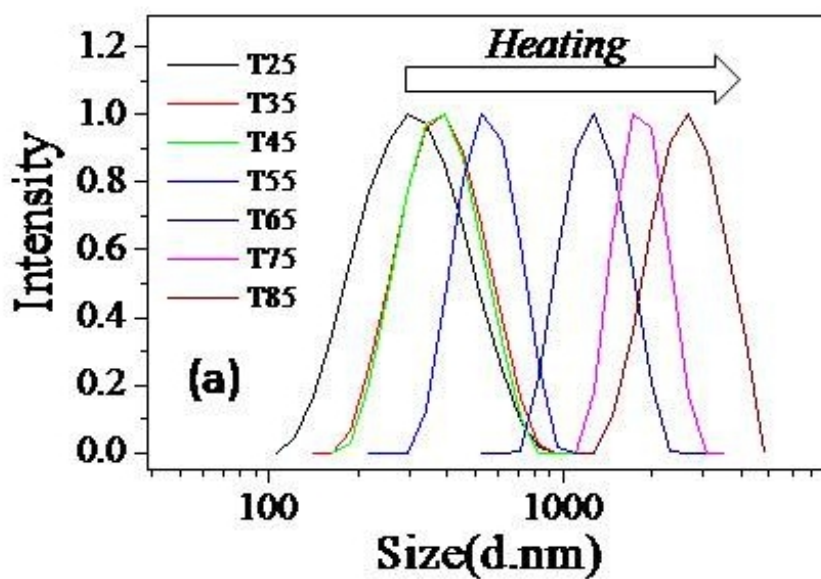


Figure SF-9. DLS data of amphiphile **1** (10^{-4} M) complexed with ATP (300 mM) (a) heating cycle (b) cooling cycle.

Note: From the plot of heating cycle it is evident that size of the aggregates increases from 300 nm to 2.0 μm upon heating. This indicates that amphiphile **1** in presence of ATP undergoes aggregation or precipitation at higher temperature (above LCST). While, upon cooling the size of the aggregate does not regain their original size indicating that the complex of amphiphile **1** and ATP is highly stable.

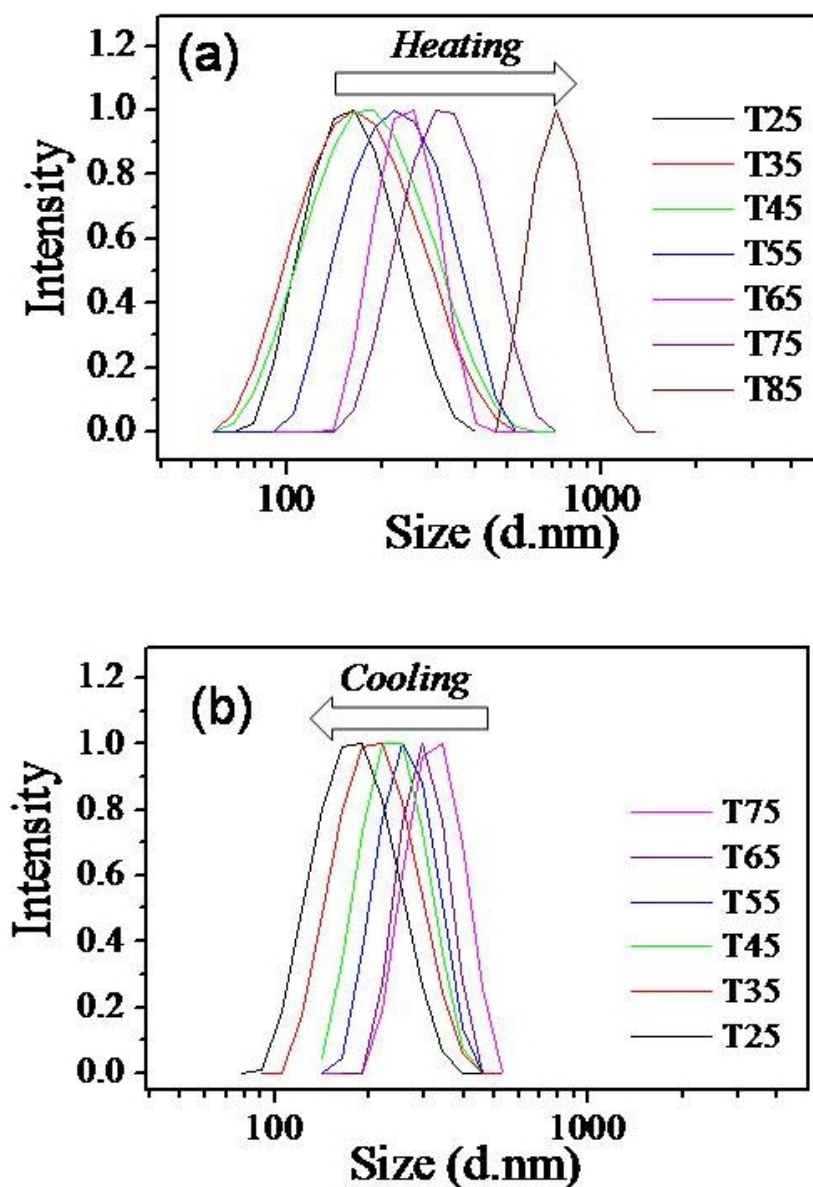


Figure SF-10. DLS data of amphiphile **1**(10^{-4} M) complexed with Pi (300 mM) (a) heating cycle (b) cooling cycle.

Note: From the plot of heating cycle it is evident that size of the aggregates increases from 150 nm to 700 nm upon heating. This indicates that amphiphile **1** in presence of inorganic phosphate anion undergoes aggregation or precipitation at higher temperature (above LCST). While, upon cooling the size of the aggregate reverts back to its original size indicating that the complex of amphiphile **1** and Pi is less stable.

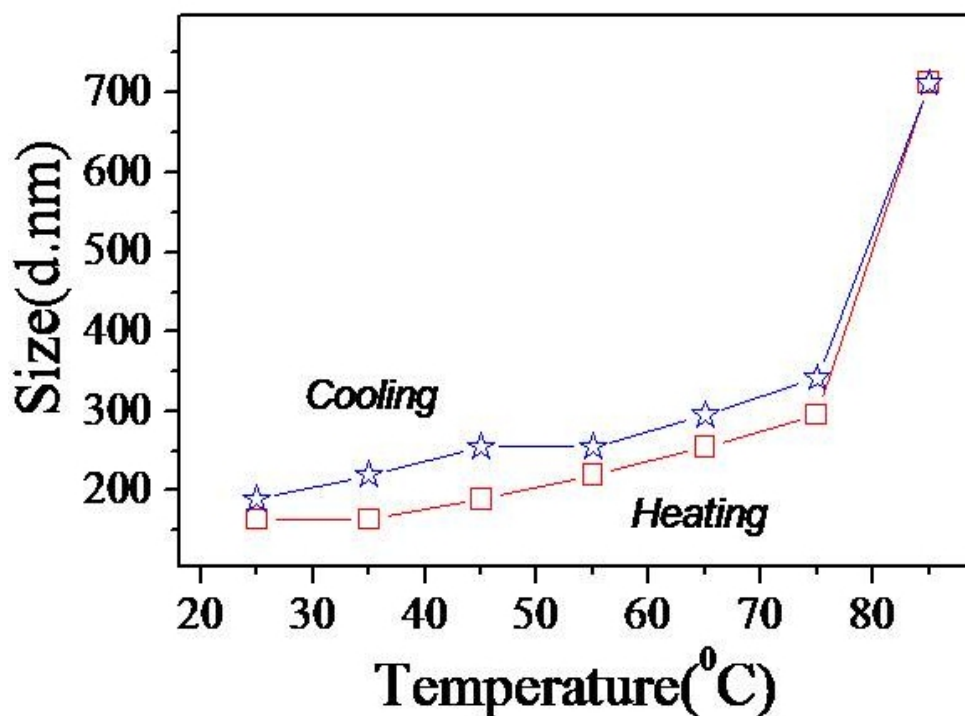


Figure SF-11. Plot of hydrodynamic diameter of amphiphile **1** against temperature obtained from heating and cooling cycle of Pi.

Note: From the plot it is evident that the rate by which aggregates are formed upon heating is similar to the rate by which the aggregates disassemble upon cooling, indicates that both heating and cooling cycle follow same kinetic path.

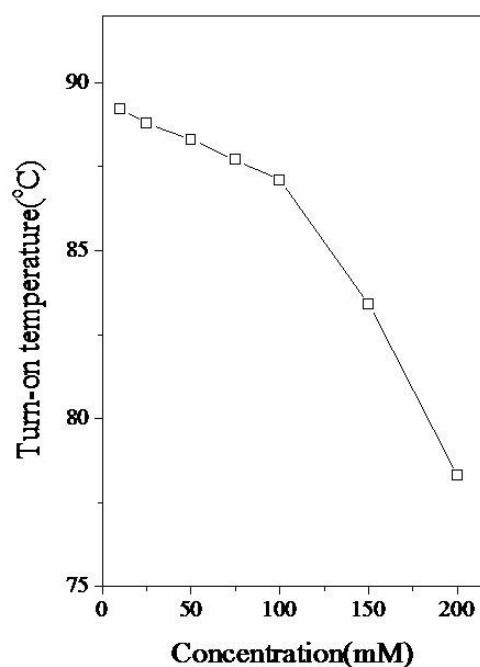
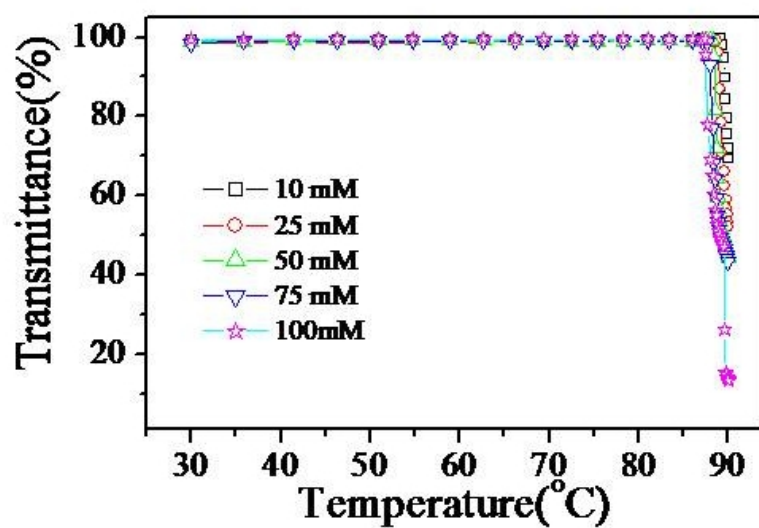
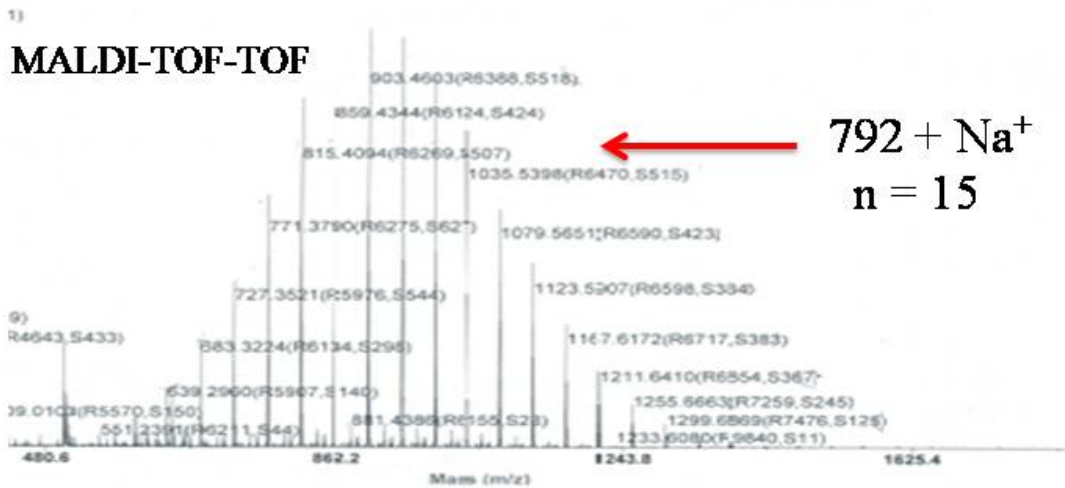
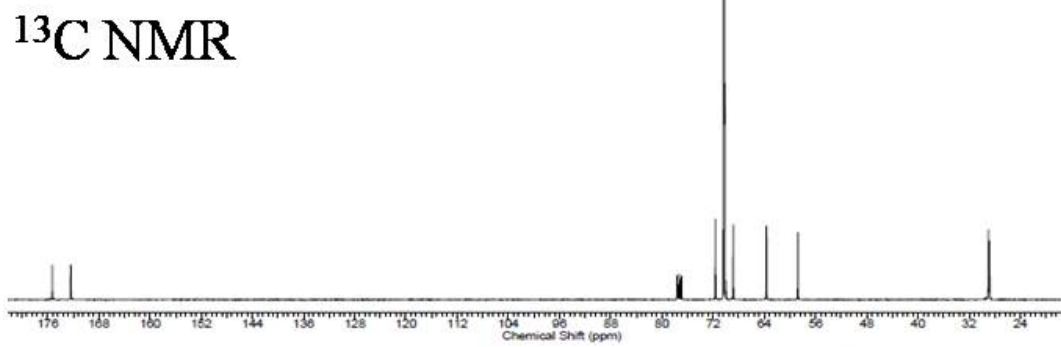
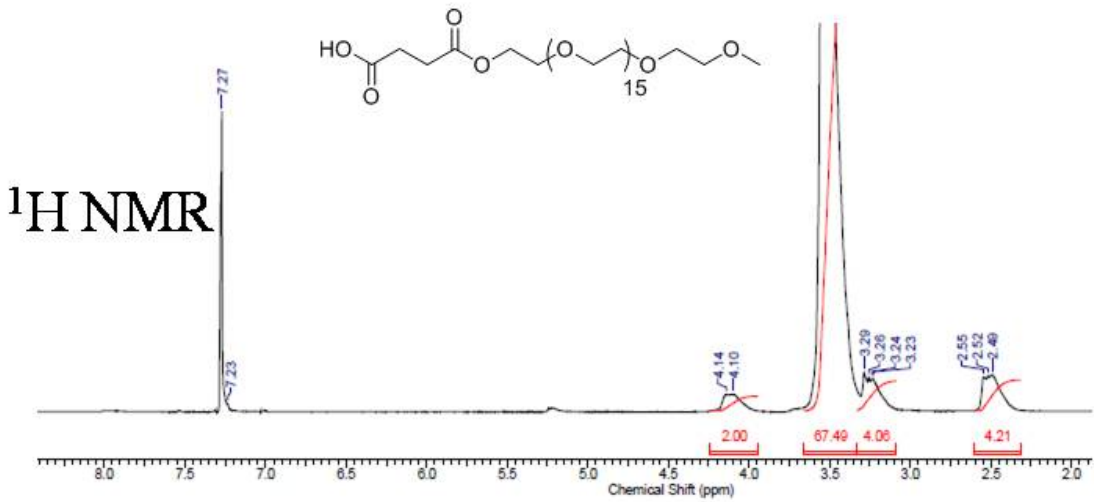


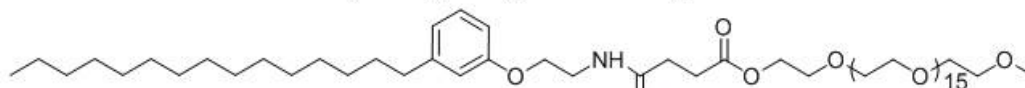
Figure SF-12. Plot of turn-on temperature of amphiphile 1 in presence of various concentration of ATP.

Note: From the plot it is evident that the detection limit of amphiphile 1 for ATP is 100 mM (break point) .

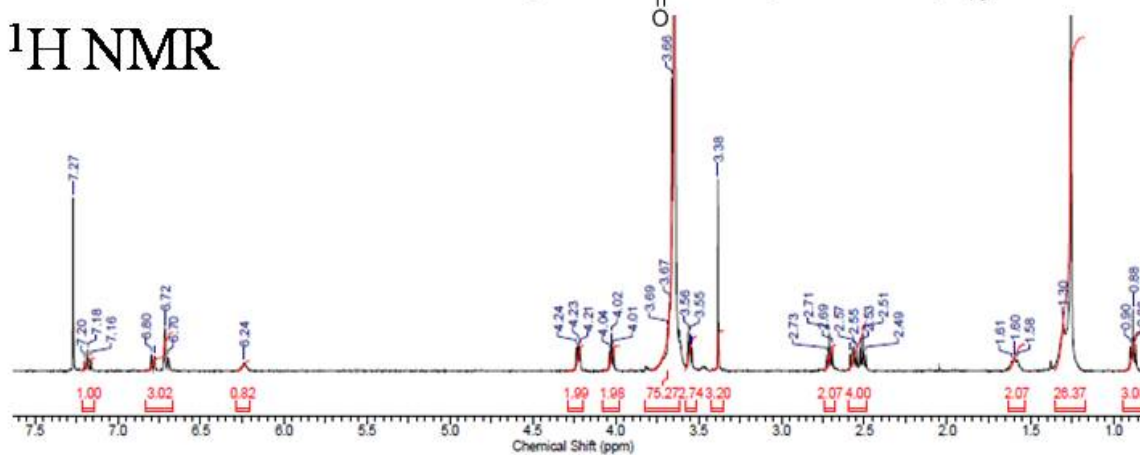
PEG-750-Acid



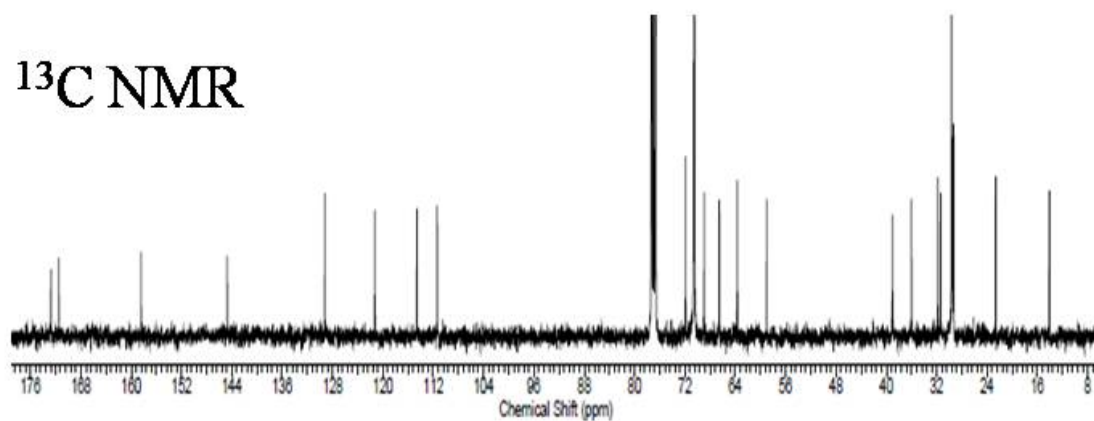
PDP-PEG 750 (amphiphile 1)



^1H NMR



^{13}C NMR



MALDI-TOF-TOF

